http://dx.doi.org/10.11142/jicems.2013.2.2.184

Performance Improvement of Slotless SPMSM Position Sensorless Control in Very Low-Speed Region

Takurou Iwata*, Shigeo Morimoto*, Yukinori Inoue* and Masayuki Sanada*

Abstract – **This paper proposes a method for improving the performance of a position sensorless control system for a slotless surface permanent magnet synchronous motor (SPMSM) in a very low-speed region. In position sensorless control based on a motor model, accurate motor parameters are required because parameter errors would affect position estimation accuracy. Therefore, online parameter identification is applied in the proposed system. The error between the reference voltage and the voltage applied to the motor is also affect position estimation accuracy and stability, thus it is compensated to ensure accuracy and stability of the sensorless control system. In this study, two voltage error compensation methods are used, and the effects of the compensation methods are discussed. The performance of the proposed sensorless control method is evaluated by experimental results.**

Keywords: **Slotless SPMSM, Sensorless control, Online parameter identification, Voltage error compensation**

1. Introduction

The permanent magnet synchronous motor (PMSM) is used in a number of applications due to its high power, high efficiency, and wide operating speed range. The control system for a PMSM requires information on the rotor position and speed. To detect this information, a position sensor is frequently used for control. In order to downsize, reduce the cost of sensors, and improve reliability, position sensorless control has been studied in several papers [1]-[5].

The amplitude of back-electromotive force is proportional to the rotor speed, and a sensorless control system utilizing electromotive force (EMF) does not work well in a low-speed region because the signal-to-noise ratio of the back-EMF amplitude decreases as the rotor speed decreases.

In a position sensorless control system based on a motor model, any errors in the motor parameters would reduce estimation accuracy. To improve estimation accuracy in a low-speed region, accurate motor parameters are required. Therefore, the online parameter identification methods have been proposed [6]-[9]. Another factor is the voltage error caused by the dead-time of the inverter, which reduces estimation accuracy in such a system. Voltage error compensation and dead-time compensation methods have also been reported [8], [9]. In this paper, a model based sensorless control system for a slotless SPMSM that has a maximum speed of 40,000 min^{-1} is proposed. We intended to expand the operating speed range in the very low-speed region. The target rotating speed is set to less than 80min^{-1}, which corresponds to 0.2% of the maximum speed. The proposed sensorless control system is based on the estimation of the extended EMF [5], and it has features of the online parameter identification and the voltage error compensation. The experimental results show the effectiveness of the proposed sensorless control system.

* Dept. of Electrical and Information Systems, Osaka Prefecture University, Japan. (s0110iwata@eis.osakafu-u.ac.jp, morimoto@eis.osakafu-u.ac.jp, inoue@eis.osakafu-u.ac.jp, sanada@eis.osakafu-u.ac.jp)

Received 15 April 2013 ; Accepted 1 May 2013

2. Sensorless Control System

2.1 Model of PMSM for Sensorless Control

An electrical model of the PMSM in the reference frame is given by

$$\begin{bmatrix} v_d \\ v_q \end{bmatrix} = \begin{bmatrix} R_a + pL_d & -\omega L_q \\ \omega L_d & R_a + pL_q \end{bmatrix} \begin{bmatrix} i_d \\ i_q \end{bmatrix} + \begin{bmatrix} 0 \\ \omega \Psi_a \end{bmatrix} \quad (1)$$

where v_d and v_q are the respective d- and q-axis terminal voltages, i_d and i_q are the respective d- and q-axis armature currents, R_a is the armature resistance, L_d and L_q are the respective d- and q-axis inductances, Ψ_a is the stator flux linkage by the rotor magnet, ω is the electrical angular speed, and $p=d/dt$.

Fig. 1 shows the relation of the reference frames. A d-q reference frame, which is synchronously rotating at the electrical angular speed ω, is generally used for the PMSM control system. However, due to the lack of a position sensor in a sensorless control system, the d-q reference

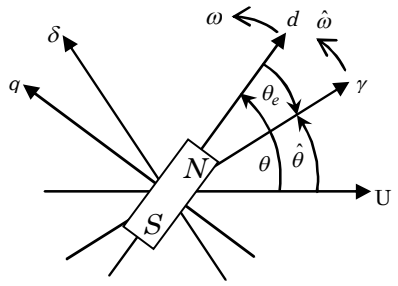

Fig. 1. Definition of the estimated frame

frame is not available. Therefore, the estimated rotating frame, γ-δ frame, which lags the d-q frame by a position error θ_e, is used. The PMSM model in the γ-δ frame derived from (1) is shown below [5],[7],[8],

$$\begin{bmatrix} v_\gamma \\ v_\delta \end{bmatrix} = \begin{bmatrix} R + pL_d & -\omega L_q \\ \omega L_q & R + pL_d \end{bmatrix} \begin{bmatrix} i_\gamma \\ i_\delta \end{bmatrix} + \begin{bmatrix} e_\gamma \\ e_\delta \end{bmatrix} \tag{2}$$

$$\begin{bmatrix} e_\gamma \\ e_\delta \end{bmatrix} = E_{ex} \begin{bmatrix} -\sin\theta_e \\ \cos\theta_e \end{bmatrix} + (\hat{\omega} - \omega) L_d \begin{bmatrix} -i_\delta \\ i_\gamma \end{bmatrix} \tag{3}$$

$$E_{ex} = \omega \{ (L_d - L_q) i_d + \Psi_a \} - (L_d - L_q)(p i_q) \tag{4}$$

where v_γ and v_δ are the respective γ- and δ-axis terminal voltages, i_γ and i_δ are the respective γ- and δ-axis armature currents, e_γ and e_δ are the respective γ- and δ-axis extended EMFs, R is the winding resistance, and $\hat{\omega}$ is the estimated electrical angular speed.

2.2 Position and Speed Estimation Method

Based on the motor model of (2), the disturbance observer to estimate the extended EMF e_γ and e_δ are given by,

$$\hat{e}_\gamma = \frac{g}{s+g} \{ v_{\gamma 1} - (L_d s + R) i_\gamma \} \ ,$$
$$\hat{e}_\delta = \frac{g}{s+g} \{ v_{\delta 1} - (L_d s + R) i_\delta \} \tag{5}$$

where ^ represents the estimated value. To remove the interference component between the γ-axis and δ-axis, the voltage components shown in (6) are created and remove the interference component in advance.

$$v_{\gamma 1} = v_\gamma + \hat{\omega} L_q i_\delta, \quad v_{\delta 1} = v_\delta - \hat{\omega} L_d i_\gamma \tag{6}$$

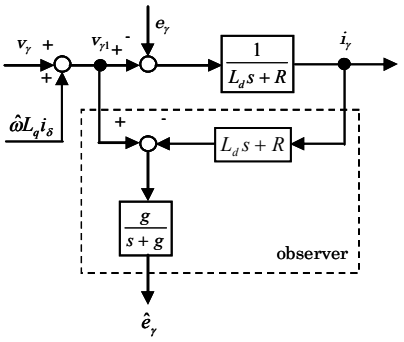

Fig. 2. Block diagram of the disturbance observer for estimating e_γ

The equivalent block diagram of the disturbance observer

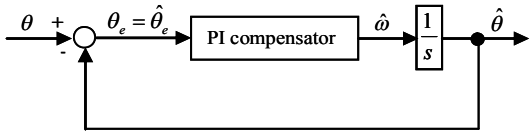

Fig. 3. Equivalent block diagram of the position and speed estimator

for estimating e_γ is shown in Fig. 2, where g represents the gain of the observer. The δ-axis component of the extended EMF e_δ is estimated in the same way as e_γ.

Assuming that the estimated speed $\hat{\omega}$ is approximately equal to the actual speed ω, (3) is transformed into (7) and the estimated position error $\hat{\theta}_e$ can be obtained.

$$\hat{\theta}_e = \tan^{-1}\left(-\frac{\hat{e}_\gamma}{\hat{e}_\delta} \right) \tag{7}$$

The position and speed are estimated by compensation to converge the estimated position error to zero. The equivalent block diagram of the position and speed estimator is shown in Fig. 3, and the estimator can be regarded as a feedback control system. Here, proportional and integral compensator is used as a compensator.

2.3 Online Parameter Identification

Accurate parameters are required for position sensorless control based on a motor model. Online parameter identification is used to improve estimation accuracy. The resistance R is identified in the proposed system.

The recursive least squares (RLS) method is used in the identification algorithm. The general formula of the algorithm is represented as follows,

$$Y(k)=\Theta^T(k)Z(k) \tag{8}$$

$$\hat{\Theta}(k)=\hat{\Theta}(k-1)+\frac{\boldsymbol{P}(k-1)Z(k)}{\lambda+Z^T(k)\boldsymbol{P}(k-1)Z(k)}\left(Y(k)-Z^T(k)\hat{\Theta}(k-1)\right) \tag{9}$$

$$\boldsymbol{P}(k)=\frac{1}{\lambda}\left(\boldsymbol{P}(k-1)-\frac{\boldsymbol{P}(k-1)Z(k)Z^T(k)\boldsymbol{P}(k-1)}{\lambda+Z^T(k)\boldsymbol{P}(k-1)Z(k)}\right) \tag{10}$$

where Θ is the parameter coefficient vector, $\hat{\Theta}$ is the estimated parameter coefficient vector, $\boldsymbol{P}$ is the covariance matrix, Y is the output, Z is the input vector, and λ is the forgetting factor given by $\lambda < 1$.

The voltage equation considering the voltage error of the inverter derived from (2) is given by

$$\begin{bmatrix} v_{\gamma\_ref} \\ v_{\delta\_ref} \end{bmatrix}=\begin{bmatrix} R+pL_d & -\omega L_q \\ \omega L_q & R+pL_d \end{bmatrix}\begin{bmatrix} i_\gamma \\ i_\delta \end{bmatrix}+\begin{bmatrix} e_\gamma \\ e_\delta \end{bmatrix}+\Delta V\begin{bmatrix} D_\gamma \\ D_\delta \end{bmatrix} \tag{11}$$

where v_{γ_ref} and v_{δ_ref} are the γ- and δ-axis reference voltages, ΔV is the amplitude of the voltage error, and D_γ and D_δ are state variables dependent on the rotor position and the phase currents, respectively.

The identification model of R is represented as follows [7],

$$Y(k)=v_{\delta\_ref}(k-1)-L_d\omega(k-1)i_\gamma(k-1)-\Psi_a\omega(k-1)-\Delta V D_\delta(k-1) \tag{12}$$

$$Z(k)=i_\delta(k-1) \tag{13}$$

$$\Theta(k)=R \tag{14}$$

This identification model is derived from the δ-axis voltage equation of (11). The identified value $\hat{R}$ is used in the proposed system.

2.4 Voltage Error Compensation of the Inverter

Since a voltage error caused by the dead-time of the inverter exists between the reference voltage and the voltage applied to the motor, such voltage error has to be compensated. Two voltage error compensation methods are used in this paper: compensation method 1 is the conventional voltage error compensation method, while compensation method 2 is the proposed method.

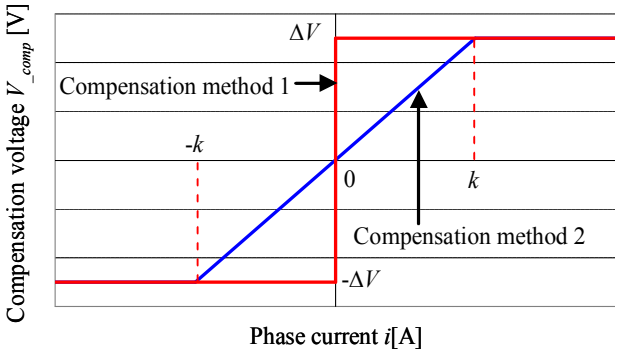

Fig. 4. Compensation methods

Compensation method 1 is given by (15) and compensation method 2 is given by (16),

$$V_{\_comp}=\Delta V\times\mathrm{sgn}(i) \tag{15}$$

$$V_{\_comp}=\frac{\Delta V}{2}\{\mathrm{sgn}(i+k)+\mathrm{sgn}(i-k)\}+\frac{\Delta V}{2k}i\{\mathrm{sgn}(i+k)-\mathrm{sgn}(i-k)\} \tag{16}$$

where k is a constant and sgn(i) is the sign function (sgn(i) $=i/|i|$).

The compensation methods are shown in Fig. 4. Compensation method 1 compensates the voltage according to the polarity of the phase current, while compensation method 2 compensates the voltage according to the phase current value. Method 1 is sensitive to the polarity of the current at low currents, and the voltage seems to be excessively compensated. On the other hand, there are not such problems in Method 2. Then, the influence is a little even if noise is included in the detected current. The values of ΔV and k affect the performance of sensorless control. Here, they are set to ΔV=0.05V, k=0.1A.

3. Experimental Results

3.1 Experimental System

Fig. 5 is a block diagram of the proposed sensorless control system, and Table 1 lists the parameters used in the experimental system. In the speed regulator, the reference currents are produced by a PI compensator according to the speed error. In the current regulator, the reference voltages are created by a PI compensator due to the current error. The operating condition is a no-load, and the DC link voltage is set a low value in the experiment.

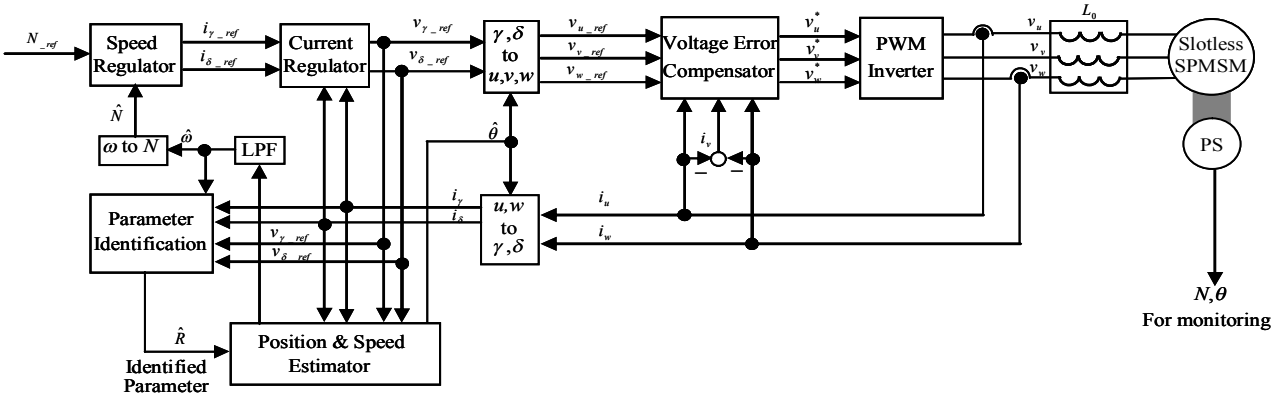

Fig. 5. Block diagram of the experimental system

3.2 Effectiveness of Online Parameter Identification

Table 1. Parameters of the experimental system

Number of pole pairs P_n	1
Magnet flux linkage Ψ_a	0.00415 Wb
d-axis inductance L_d	77 μH
q-axis inductance L_q	79 μH
External inductance L_0	120 μH
Resistance R	0.965 Ω
Maximum speed	40,000 min^{-1}
DC link voltage	4 V
PWM carrier frequency	12 kHz
Dead-time of the inverter	1 μs

To verify the effectiveness of online parameter identification, the resistances used for the position and speed estimator are 0.965 Ω, which is the measured value, and 0.992 Ω, which is the average value of the identification value when the reference speed is 80 min^{-1}, and the online identification value. In this experiment, compensation method 2 is applied as the voltage error compensation. Fig. 6(a) and (b) show the average value of the absolute value of the estimation position error, and the difference between the maximum and minimum values of the estimation position error, respectively. As shown in Fig. 6, the estimation position error increases as the speed decreases and there is almost no difference with respect to the difference of the resistance value up to 150 min^{-1}. Moreover, when the reference speed is less than 150 min^{-1}, setting the resistance value to 0.992 Ω gives a smaller estimation position error than setting the value to 0.965 Ω. In addition, setting the resistance value to the identification value gives the smallest position estimation error. Therefore, the validity of online identification of the resistance R is confirmed.

3.3 Effectiveness of Voltage Error Compensation

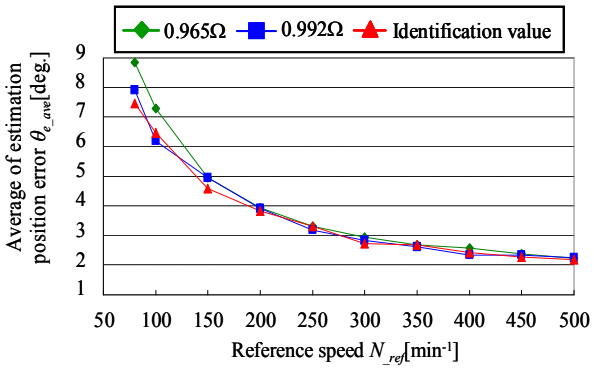

(a) Average of estimation position error

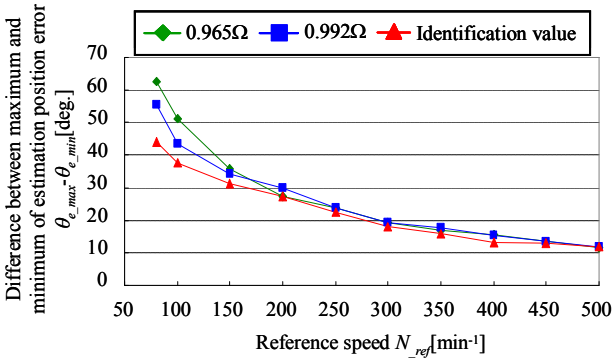

(b) Difference between the maximum and minimum values of the estimation position error

Fig. 6. Comparison of performances using identification of R

Figs. 7 and 8 show the experimental results when online parameter identification and both voltage error compensation methods are used. Fig. 7(a) and (b) show the average value of the absolute value of the estimation position error and the difference in the maximum and minimum values of the estimation position error,

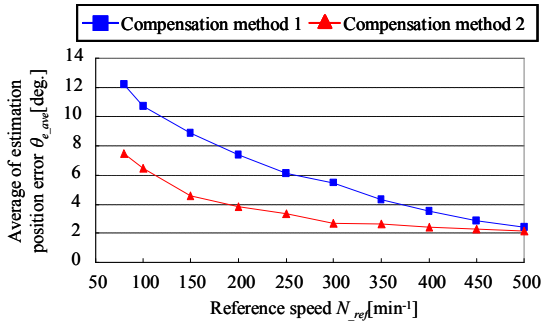

(a) Average of estimation position error

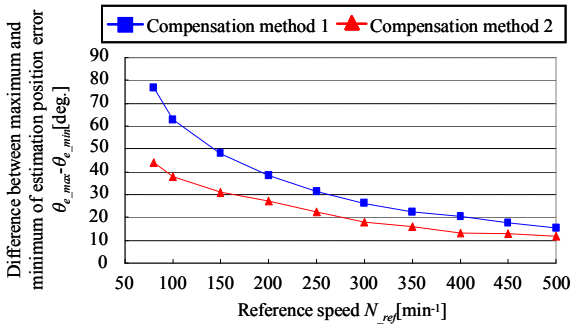

(b) Difference between the maximum and minimum values of the estimation position error

Fig. 7. Comparison of performance differences of the voltage compensation methods

respectively. Fig. 8 shows the u-phase compensation voltage and the u-phase current at 80 min^{-1} when compensation methods 1 and 2 are applied. Fig. 7 shows a larger estimation position error when compensation method 1 is applied than when compensation method 2 is applied. This is because compensation method 1 is thought to compensate the voltage beyond the actual voltage error of the inverter when the phase current is near 0 A, as show in Figure 8. Compensation method 2 contributes to an improvement in accuracy of the estimation position error at a very low-speed.

3.4 Lowest Operating Speed

Fig. 9 shows the maximum, minimum and average values of the lowest operating speed, where the lowest operating speed is the limit value of the reference speed that the system remains stable. As experimental condition, the combinations of compensation method and resistance value are given in Table 2. Each experiment is conducted five times. From Fig. 9, when using compensation method 2, setting the resistance value to 0.992 Ω gives a lower operating speed than setting the value to 0.965 Ω. In addition, setting the resistance value to the identification value gives the lowest operating speed. In the very low speed region, the sensorless control

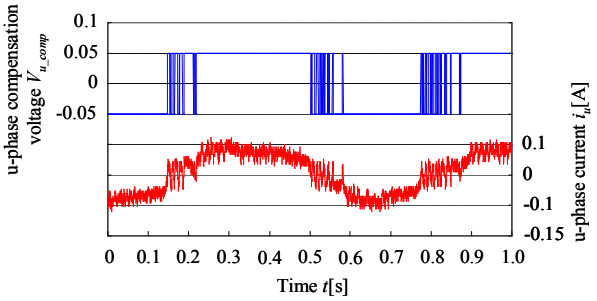

(a) u-phase compensation voltage and u-phase current applied compensation method 1

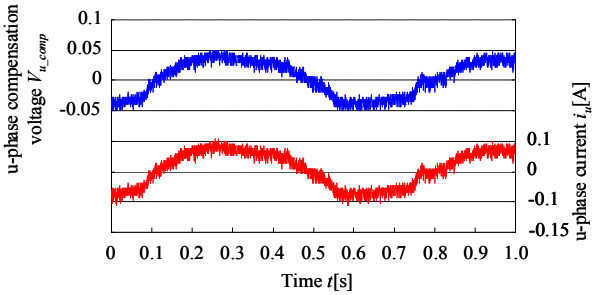

(b) u-phase compensation voltage and u-phase current applied compensation method 2

Fig. 8. Comparison of performance differences of voltage compensation methods at 80 min^{-1}

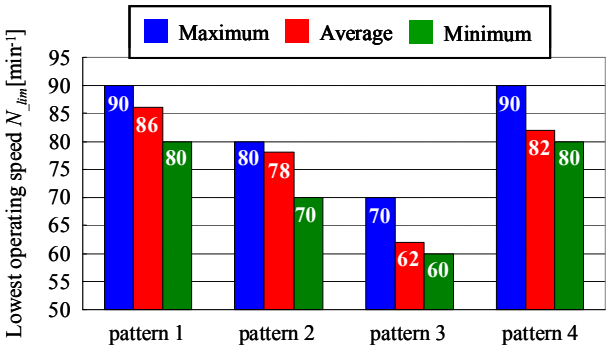

Fig. 9. Maximum, minimum and average values of the lowest operating speed

Table 2. Experimental conditions

	Compensation method	Resistance
Pattern 1	Method 2	0.965 Ω
Pattern 2	Method 2	0.992 Ω
Pattern 3	Method 2	Identification value
Pattern 4	Method 1	

is very sensitive to the resistance value. It is thought that system the identified resistance contains a wiring resistance and on-resistance of the inverter devices not only winding resistance. In addition, the influence of other parameter error seems to be included in the identified resistance. Therefore, the system will become more stable by using the

identified resistance than with the real winding resistance.

On the other hand, application of compensation method 2 gives a lower operating speed than application of compensation method 1. Only the proposed system with the identification of resistance and voltage compensation method 2 is able to expand the operating speed range to less than 80 min^{-1}, which is the target rotating speed.

4. Conclusion

This paper evaluated the validity of voltage error compensation and online parameter identification for a slotless SPMSM sensorless control system in a very low-speed region. The experimental results confirmed that online parameter identification of resistance is effective. Since compensation method 1 compensates voltage beyond the actual voltage error of the inverter, both the estimation position error and limit speed became larger. Thus, the estimation position accuracy was improved by applying compensation method 2. Only the proposed system was able to expand the operating speed range to less than 80 min^{-1}, which corresponds to 0.2% of the maximum speed of the tested slotless SPMSM.

References

[1] M. Schroedl, "Sensorless Control of AC Machines at Low Speed and Standstill Based on the "INFORM" Method," Proc. 1996 *IEEE IAS Ann. Meeting*, pp. 270-277, 1996

[2] L. Wang, and R. D. Lorenz, "Rotor Position Estimation for Permanent Magnet Synchronous Motor Using Saliency-Tracking Self-Sensing Method," Proc. 2000 *IEEE IAS Ann. Meeting*, pp. 445-450, 2000.

[3] J. H. Jang, S. K. Sul, J. I. Ha, K. Ide, and M. Sawamura, "Sensorless Drive of Surface-Mounted Permanent-Magnet Motor by High-Frequency Signal Injection Based on Magnetic Saliency," *IEEE Trans. Ind. Applicat*., vol. 39, no. 4, pp.1031-1039, 2003.

[4] J. K. Seok, J. K. Lee, and D. C. Lee, "Sensorless Speed Control of Nonsalient Permanent-Magnet Synchronous Motor Using Rotor-Position-Tracking PI Controller," *IEEE Trans. Ind. Electron*., vol. 53, no. 2, pp.399-405, 2006.

[5] S. Morimoto, K. Kawamoto, M. Sanada, and Y. Takeda, "Sensorless Control Strategy for Salient-pole PMSM Based on Extended EMF in Rotating Reference Frame," *Proc. 1996 IEEE IAS Ann. Meeting*, pp. 445-450, 2000.

[6] S. Ichikawa, M. Tomita, S. Doki, and S. Okuma, "Sensorless Control of Permanent-Magnet Synchronous Motor Using Online Parameter Identification Based on System Identification Theory," *IEEE Trans. Ind. Electron.*, vol. 53, no. 2, pp.363-372, 2006.

[7] Y. Inoue, Y. Kawaguchi, S. Morimoto, and M. Sanada, "Performance Improvement of Sensorless IPMSM Drives in Low-speed Region Using Online Parameter Identification," *Proc. IEEE-ECCE*, pp. 1933-1938, 2009.

[8] Y. Inoue, K. Yamada, S. Morimoto, and M. Sanada, "Effectiveness of Voltage Error Compensation and Parameter Identification for Model-Based Sensorless Control of IPMSM," *IEEE Trans. Ind. Applicant*., vol. 45, no. 1, pp. 213-221, 2009.

[9] T. Fukumoto, H. Hamane, and Y. Hayashi, "Performance Improvement of the IPMSM Position Sensor-less Vector Control System by the On-line Motor Parameter Error Compensation and the Practical Dead-Time Compensation," *Proc. PCC-Nagoya 2007*, pp. 314-321, 2007.

Takurou Iwata received the B.E. and M.E. degrees from Osaka Prefecture University, in 2011 and 2013, respectively. He was involved in the study on the sensorless drive system for permanent magnet synchronous motors at Osaka Prefecture University. He is currently with Kawasaki Heavy Industries, Kobe, Japan.

Shigeo Morimoto received the B.E., M.E., and Ph.D. degrees from Osaka Prefecture University, in 1982, 1984, and 1990, respectively. Since 1988, he has been with the Graduate School of Engineering, Osaka Prefecture University, where he is currently a Professor. His research interests include permanent magnet synchronous machines, reluctance machines and their control systems.

Yukinori Inoue received the B.E., M.E., and Ph.D. degrees from Osaka Prefecture University, in 2005, 2007, and 2010, respectively. Since 2010, he has been with the Graduate School of Engineering, Osaka Prefecture University, where he is currently an Assistant Professor. His research interests include control of electrical drives, particularly DTC and position-sensorless control of PMSMs.

Masayuki Sanada received the B.E., M.E., and Ph.D. degrees from Osaka Prefecture University, in 1989, 1991, and 1994, respectively. Since 1994, he has been with the Graduate School of Engineering, Osaka Prefecture University, where he is currently an Associate Professor. His research interests include permanent-magnet motors for direct-drive applications, their control systems, and magnetic field analysis.